Journal of Thermal Analysis and Calorimetry, Vol. 85 (2006) 2, 361–368

APPLICATION OF HIGH PRESSURE DSC TO THE KINETICS OF FORMATION OF METHANE HYDRATE IN WATER-IN-OIL EMULSION

D. Dalmazzone[1*], *N. Hamed*[1], *Christine Dalmazzone*[2] *and L. Rousseau*[2]

[1]Ecole Nationale Supérieure de Techniques Avancées, Laboratoire Chimie et Procédés, 32 Boulevard Victor 75739 Paris Cedex 15, France
[2]Institut Français du pétrole, Division Chimie et Physico-chimie Appliquées, 1–4 Avenue Bois Préau 92852 Rueil Malmaison Cedex, France

A micro DSC analyzer fitted with special high-pressure vessels was used to investigate the kinetics of methane hydrate formation in the water phase dispersed as a stable emulsion in deep offshore drilling fluids. At high sub-cooling conditions, the peak of hydrate formation is perfectly visible and regular-shaped, and could be fitted by a Gaussian law. The average time for hydrate crystallization of the water droplets' population was represented as a logarithmic function of the inverse of absolute temperature. At low sub-cooling conditions, the formation appears confused with the baseline; the amount of hydrate formed was thus measured from its enthalpy of dissociation, after periods of formation of variable duration.

Keywords: *DSC, kinetics, methane hydrates, water-in-oil emulsion*

Introduction

Thermal and calorimetric analyses have long been known to be particularly suitable for investigating phase transitions involving water, which generally lead to strong enthalpy changes. This is the case of the crystallization of gas hydrates, which are solid structures formed of small molecules, such as light hydrocarbons, enclathrated in a lattice of water molecules stabilized by Van der Waals interactions. According to the structure, hydrate formation may release from 1.5 to 3 times more energy than the freezing of ice. When the transition occurs in a finely dispersed water phase, where optic or spectroscopic observations are difficult, the heat evolved becomes the most easily detectable evidence of hydrate formation.

Such dispersed hydrate formation may occur in the drilling fluids that are used in offshore drilling operations. In those fluids, water droplets, 1 to 10 micrometer in diameter, are dispersed in the form of an emulsion in a mineral oil, in which the gases readily dissolve and are thus available in great amount to form hydrates at the oil–water interface. The huge specific area of the interface is expected to allow much faster hydrate crystallization than in the bulk phase, resulting in severe threats towards the safety and economy of drilling operations. Studying the formation of hydrates in drilling fluids by usual techniques is made difficult by the properties of such fluids: they are opaque, corrosive, and very viscous. Furthermore, to reproduce the thermodynamic conditions of deep offshore, measurements must be conducted at pressures exceeding 30 MPa.

This paper presents the results of measurements of the kinetics of methane hydrate formation in the water phase dispersed in drilling fluids, using specially designed high-pressure DSC vessels.

Background

Applications of DSC to hydrates

Since the 1980's, calorimetry has mainly been used in the study of clathrate hydrates for the measurement of thermal properties, such as enthalpies of dissociation and heat capacities [1–3]. The recent development of more sensitive and faster equipments opened the way to new applications. Differential scanning calorimetry (DSC) was first applied to the study of hydrates by Koh *et al.* [4], who performed experiments on a model hydrate at ambient pressure, using DSC to quantify and compare the effect of various kinetic inhibitors. The same technique, which had been formerly utilized for studying the mechanisms of crystallization and melting of ice in water-in-oil emulsions [5], was extended by Fouconnier *et al.* to the study of the formation and dissociation of model hydrates in water-in-oil emulsions [6, 7]. DSC coupled with X-rays diffraction (XRDT) was applied as a complementary technique to elucidate the complex thermal events that were observed [6].

* Author for correspondence: Didier.Dalmazzone@ensta.fr

1388–6150/$20.00

Akadémiai Kiadó, Budapest, Hungary
Springer, Dordrecht, The Netherlands

The first application of high-pressure DSC (HP-DSC) to gas hydrates was developed to characterize the thermodynamic stability limits of methane and natural gas hydrates in solutions of inhibitors [8]. Bulk solutions, as well as water-in-oil emulsions, were studied, and the technique found an interesting industrial application in deep offshore drilling fluids [9–13]. HP-DSC has then been used to study the (hydrate+salt+liquid+vapor) phases behavior in highly concentrated salt solutions [14, 15].

Drilling fluids

Drilling fluids used in the oil industry have several essential functions [16]. They have to transport drill cuttings in suspension back to the surface, to lubricate and to cool the drill bit, and also to maintain pressure in the well, preventing oil or gas blowouts. Generally, drilling fluids are of two types:

- water-based fluids, composed of water and various additives like electrolytes, clays, polymers and solid weighing agents,
- oil-based fluids, composed of brine-in-oil emulsion with lipophilic clays and polymers, and solid weighing agents.

Deep offshore drilling operations are now a reality and ultra deep offshore drilling (>4000 ft) appears as an objective, though difficult and expensive to achieve. Temperature and pressure conditions encountered at these water depths (down to 272 K and up to 40 MPa) require a specific adaptation of the drilling fluids, because of the likely formation of gas hydrates. The occurrence of gas hydrate formation in deep offshore drilling operations has been described [17]. The formation of solid crystals of gas hydrates into the fluid may block the lines or the annular and cause strong damages to the rig equipment as well as serious safety problems to operators. Gas hydrate formation is prevented by adding thermodynamic inhibitors to drilling fluids formulations [18]. The use of kinetic inhibitors was evocated in a few recent papers as an alternate way of prevention [19, 20].

Kinetics of crystallization in dispersed systems

Like any crystallization process, gas hydrate formation proceeds in two steps: the nucleation followed by the crystal growth.

The nucleation corresponds to the formation of nuclei, also called 'critical germs', into the solution. Generally, three types of nucleation are considered [21]: the primary homogeneous nucleation that occurs spontaneously, the primary heterogeneous nucleation that is induced by foreign solid particles and the secondary nucleation that is induced by already formed crystals. Nucleation relies on a probabilistic scheme, and requires that a thermodynamic potential barrier be overcome. This results in two consequences: first, the liquid has to be cooled below the bulk temperature of equilibrium to crystallize (under-cooling or sub-cooling); second, the rate of appearance of critical germs in a given sample depends on the sub-cooling degree and the sample size. In the literature on hydrates kinetics, most of the authors underlined the great experimental difficulties for obtaining reproducible results when studying hydrates nucleation from liquid water. Some authors chose to overcome the problem by studying hydrate nucleation from melting ice [22]. Sloan and Fleyfel [23] proposed in 1991 a molecular mechanism to explain hydrates nucleation from ice.

Major works concerning hydrates crystal growth were published from the eighties [24]. The main experimental parameters that govern hydrates crystal growth are the rate of gas diffusion, the interfacial area, pressure, temperature and of course, the degree of undercooling. Several models were developed for predicting hydrates kinetics [25–27] but it is worth noticing that up to date, no acceptable model exists because nucleation phenomena remain poorly understood and controlled, and models for describing crystal growth depend essentially on the experimental device.

Crystallization of ice in water-in-oil emulsions has been extensively studied using DSC [5, 28, 29]. It appeared that each droplet behaves as an isolated sample of very small size, and consequently, that the heat signal released by the crystallization of the whole population allows to get a statistical response from a unique experiment. It seems logical to expect similar results for hydrate formation in dispersed aqueous populations, even though gas hydrate crystal growth requires an additional step of gas transport, which makes the mechanism more complex than ice freezing.

Experimental

Materials and methods

Fluids

Methane, 99.9995 vol.%, was purchased from air liquide.

Oil-based drilling fluids were realized at IFP, following an industrial formulation corresponding to the global composition given in Table 1. All fluids were emulsions of a $CaCl_2$ solution dispersed into an oil phase and stabilized by an appropriate emulsifier. The oil phase also contained various solids in suspension. The brine to oil ratio was 20/80 vol%. We used three drilling fluids made from three different brines, with variable concentrations of $CaCl_2$. The detailed

Table 1 Composition of the oil-based drilling fluids

Phase	Compound	Quantity
Water-in-oil emulsion	base oil	800 mL (642 g)
	$CaCl_2$ brine	200 mL
	emulsifier	13.48 g
Solids	lime	2.60 g
	lipophilic clay	11.30 g
	fluid loss reducer	19.26 g
	weighing agent	385.00 g
	wetting agent	5.78 g

Table 2 Detailed composition of the aqueous phase in the different drilling fluids

	Fluid #1	Fluid #2	Fluid #3
Mass of water/g	195.4	192.3	188.7
Mass of $CaCl_2$/g	21.7	33.9	47.2
$CaCl_2$/mass%	10	15	20

compositions of the brine used for each fluid are given in Table 2.

The study of the stability of these emulsions at atmospheric pressure and under methane pressure was presented in a previous paper [30]. These fluids specially designed for deep offshore drilling were found extremely stable against ice and hydrate crystallization. This is the reason why we chose to study hydrate formation in real industrial fluids instead of simpler, but far less stable laboratory emulsions.

DSC microcalorimetry

The experimental set up has been described in [13]. It is based on a μDSCVII differential micro-calorimeter from Setaram. The specially designed gas-tight high-pressure vessels are made of Hastelloy C276; they have an internal volume of 0.5 cm^3 and a maximum operating pressure of 40 MPa. A gas high-pressure panel including a one-stage compressor provides gas feeding with constant regulated pressure. Cooling of the DSC furnace is performed by Peltier modules, with a circulation of refrigerated water as a cold source. The temperature range of operation is 223 to 393 K.

Before sampling, fluids were re-homogenized by vigorous agitation using an Ultra Turrax T8 homogenizer at 10 000 rpm during five minutes. Samples of fluid, 50 to 60 mg in mass, were carefully weighed in the experimental vessel with a precision of 10^{-5} g. A new sample was used for each experiment, and the reference vessel was left empty. After being inserted into the calorimetric block and connected to the gas panel, the two vessels were first purged by slow methane sweeping to evacuate the air, then pressurized to the experimental pressure and left during 30 min for gas diffusion into the fluid sample. Each run consisted in a cooling at the faster rate provided by the DSC (–5 K min^{-1}) followed by an isotherm of variable duration, at a temperature corresponding to a given under-cooling degree ΔT. Finally, the sample was heated at 1 K min^{-1} until complete dissociation of hydrates.

Results and discussion

DSC response to hydrate formation

The three fluids under study gave similar results; we thus present, in the following, curves obtained with the medium salt-concentrated Fluid #2 only. Results of formation kinetics obtained with the three fluids will be compared at the end of the paper in order to illustrate the effect of $CaCl_2$ concentration.

DSC response to hydrate formation depends greatly on the driving force for the formation, which may be expressed in terms of sub-cooling, as well as over pressure. At high driving force, i.e. for degrees of sub-cooling of 20 K or more, hydrate formation appears as a distinct and symmetrical exothermic peak. Figure 1 presents the heat flow and temperature signals recorded during a complete experiment, at 30 MPa methane pressure. The first heat flow peak is simply the response of the DSC sensor to the fast cooling. The second one is the heat released during the isothermal hydrate formation. The last signal reveals the dissociation of methane hydrate upon warming. The same experiment was repeated, at several methane pressures and several isotherm temperatures. As can be seen in Figs 2 and 3, hydrate formation peaks get wider and smoother as the sub-cooling degree decreases. At sub-cooling lower than 25 K, the peak shape changes and becomes less symmetrical, and below 20 K, hydrate formation peaks are barely distinguishable from the baseline.

Low driving force conditions are more interesting from an industrial point of view, since the temperature never falls far below 273 K at the bottom of sea. Thus, in natural conditions, the driving force for hydrate formation in drilling fluids is likely to be quite

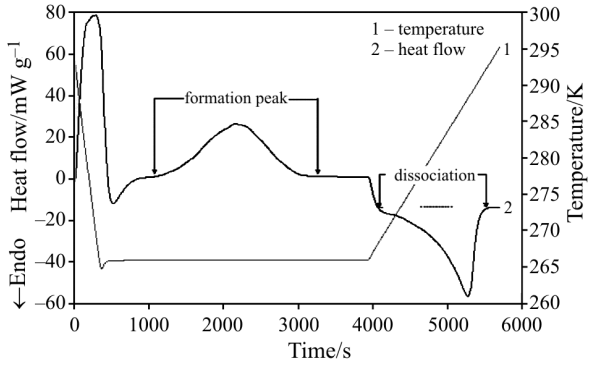

Fig. 1 Curve of formation and dissociation of methane hydrate in Fluid #2. $P(CH_4)$=30 MPa

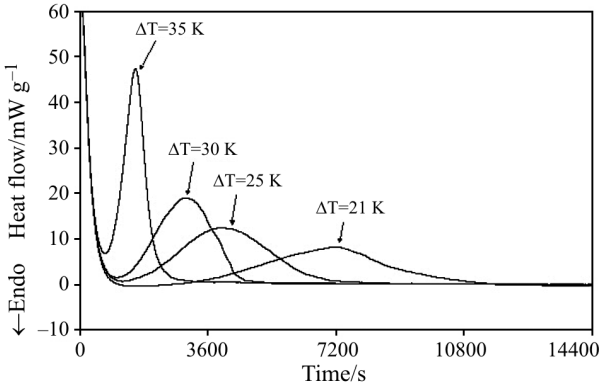

Fig. 2 Curve of methane hydrate formation during different isotherms $P(CH_4)$=22.8 MPa. Fluid #2

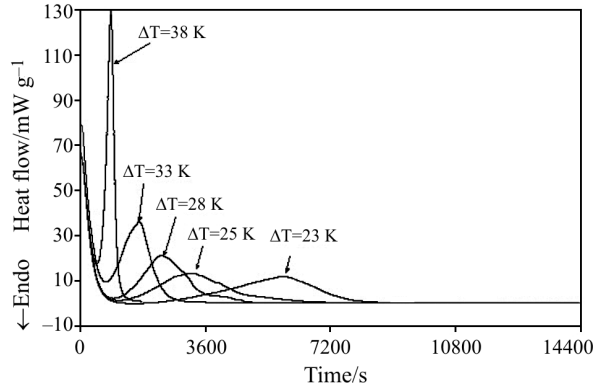

Fig. 3 Curve of methane hydrate formation during different isotherms. $P(CH_4)$=32.5 MPa. Fluid #2

low. At temperatures close to the equilibrium, formation peaks may no more be detected. Then, the only way of measuring the amount of hydrate formed during the cold isothermal period is to integrate the heat absorbed while dissociating, during the subsequent warming period. In order to follow the rate of hydrate formation *vs*. time, we performed series of experiments in which the duration of the isotherm varied from 0 (no isotherm at all) to several hours. Sample curves are presented in Fig. 4.

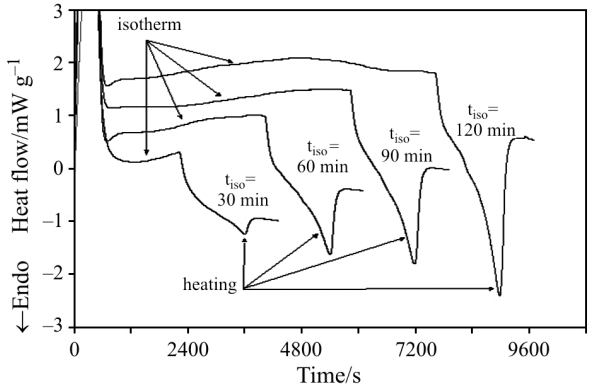

Fig. 4 Curve of methane hydrate formation and dissociation during different isotherms at low driving force. $P(CH_4)$=11 MPa. Sub-cooling: 20 K. Fluid #2

Thermodynamic limit to hydrate formation

Prior to measuring the rate of hydrate formation, it is important to know what proportion of the water contained in the sample is actually available to form hydrates. At given temperature and gas pressure, this proportion is thermodynamically limited by the salt concentration of the aqueous phase. The effect of dissolved salt on the stability limit of gas hydrate may be represented in a constant-pressure (T, x_{CaCl_2}) diagram as in Fig. 5. When a droplet of composition x_0 is cooled and kept at a constant temperature T_{iso} for an indefinite duration, hydrate forms and the water consumption causes the remaining liquid to concentrate, until the equilibrium curve is reached at x_{eq}. A common representation of the process is given by the shell model [31], as presented in Fig. 6. Notice that the assumption of a shell of hydrate forming at the interface between water and gas-rich oil has never been validated for emulsions. At all events, the thermodynamic salt effect is the same if we consider grains of hydrate forming in the solution, provided that the liquid aqueous phase may be assumed homogeneous in composition and temperature.

Previous studies [8, 9, 14] have demonstrated that the equilibrium (P, T, x) conditions of hydrates in

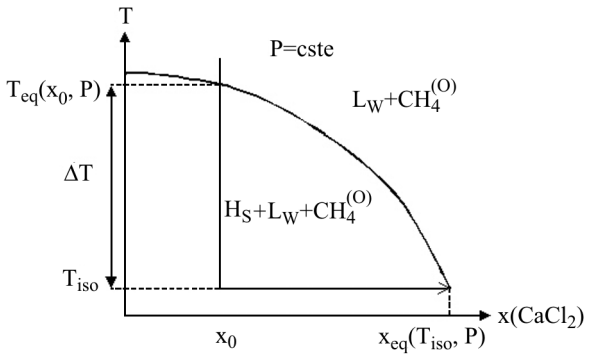

Fig. 5 Constant pressure (H_S+L_W+$CH_4^{(O)}$) equilibrium line in the (T, x_{CaCl_2}) diagram. At a given temperature T_{iso}, this line gives the maximum concentration the liquid may reach upon hydrate formation. $CH_4^{(O)}$: methane dissolved in the oil phase

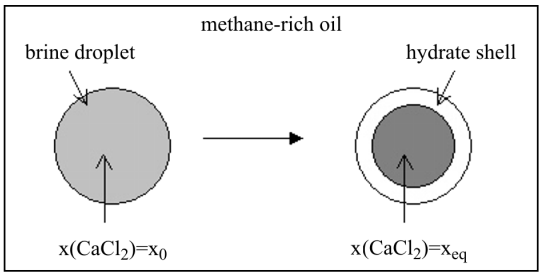

Fig. 6 The shell model. Hydrate forms at the water–oil interface, until a liquid droplet of concentration x_{eq} is surrounded by a solid hydrate shell

water-in-oil emulsions are the same as in bulk media. In emulsion, the equilibrium condition related to methane may be expressed by the double equality:

$$f_{CH_4}^{(H)} = f_{CH_4}^{(O)}$$

$$f_{CH_4}^{(O)} = f_{CH_4}^{(V)}$$

where f_{CH_4} is the fugacity of methane, and the superscripts (H), (O) and (V) refer to the hydrate, oil and vapor phase, respectively. The first equality expresses that the methane occupying the hydrate lattice is in equilibrium with the methane dissolved into the surrounding oil, and the second one expresses the assumption that methane in the oil phase is at the exact concentration of saturation. If this condition is respected, the double equality is equivalent to the single one used to express the equilibrium condition in bulk systems:

$$f_{CH_4}^{(H)} = f_{CH_4}^{(V)}$$

The concentration at equilibrium x_{eq} may thus be easily computed using classical thermodynamic models [14, 15], provided that the water and oil are totally immiscible, that the salt does not migrate into the oil phase, and that the lipophilic solids in suspension do not interfere with the water phase. The amount of water available to form hydrates is then derived from the difference $x_{eq} - x_0$.

Amount of hydrate formed vs. time

By directly integrating the well-defined peaks obtained at high driving force conditions, we determined the energy released per gram of sample as a function of time (Fig. 7). These curves give a semi-quantitative representation of the hydrate rate of formation *vs.* time. Rigorous kinetic measurements would require the knowledge of the exact enthalpy of hydrate formation at each temperature, which may differ from the formation enthalpy measured at temperatures close to the equilibrium, especially for very high ΔT. As could be expected, hydrate formation rate is extremely dependent of the sub-cooling, the time for full reaction ranging from half an hour for ΔT=38 K, to more than three hours for ΔT=21 K.

For lower driving force experiments, the amount of hydrate was determined from its enthalpy of dissociation, using the enthalpy of methane hydrate dissociation measured by Handa [2]: 54.19 kJ mol^{-1} for a hydration number of 6.00. We define the yield of hydrate formation as the ratio of the measured amount over the theoretical limit given by thermodynamic modeling. Figure 8 presents the variations of the yield, expressed in % of the theoretical maximum, *vs.* the isotherm duration, at two methane pressures for the three fluids under study. In each experiment, the hydrate formation was conducted at the same sub-cooling degree of 20 K. For this purpose the temperature of the isothermal sequence was adjusted at 20 K below the equilibrium temperature, which was computed by the same thermodynamic model from the methane pressure and salt concentration of the brine. Table 3 gathers the pressure and temperature conditions of the experiments.

Discrete yield/time plots obtained from low driving force experiments (Fig. 8) exhibit the same general S-shape as the high driving force continuous curves (Fig. 7). In both series of experiments, it may be observed that the delay for the beginning of hydrate formation depends strongly on the methane pressure. However, when formation is initiated, its rate seems relatively independent of the pressure at given salt concentration and sub-cooling degree.

The effect of salt concentration on formation kinetics is also evidenced. This is an important point since drilling fluid producers adapt the salinity of the water phase to the drilling conditions (depth, temperature) in order to comply with hydrate inhibition requirements. At the same sub-cooling degree and gas pressure, the more concentrated the solution, the lowest the rate of formation, and the longest the induction period.

Another observation is that the maximum yield reached is less than 100% and varies with the concen-

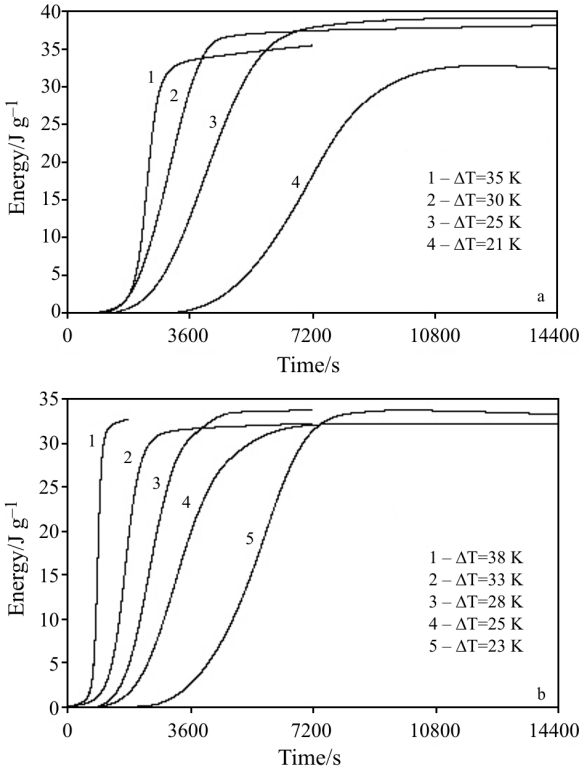

Fig. 7 Energy released per gram of sample as a function of time for different isotherms. Fluid #2. a – $P(CH_4)$=22.8 MPa; b – $P(CH_4)$=32.5 MPa

Table 3 (P, T) conditions of experiments presented in Fig. 8. Equilibrium temperatures T_{eq} are modeling results. The temperature of the isothermal sequence T_{iso} was adjusted so that $\Delta T \cong 20$ K

$P(CH_4)$/MPa	Fluid #1		Fluid #2		Fluid #3	
	T_{eq}/K	T_{iso}/K	T_{eq}/K	T_{iso}/K	T_{eq}/K	T_{iso}/K
11	282.35	262.4	279.35	259.4	273.84	253.8
20	287.30	267.3	282.45	262.5	275.64	255.6
30	290.25	270.3	285.55	265.6	278.70	258.7
40	291.92	271.9	287.65	267.7	280.87	260.9

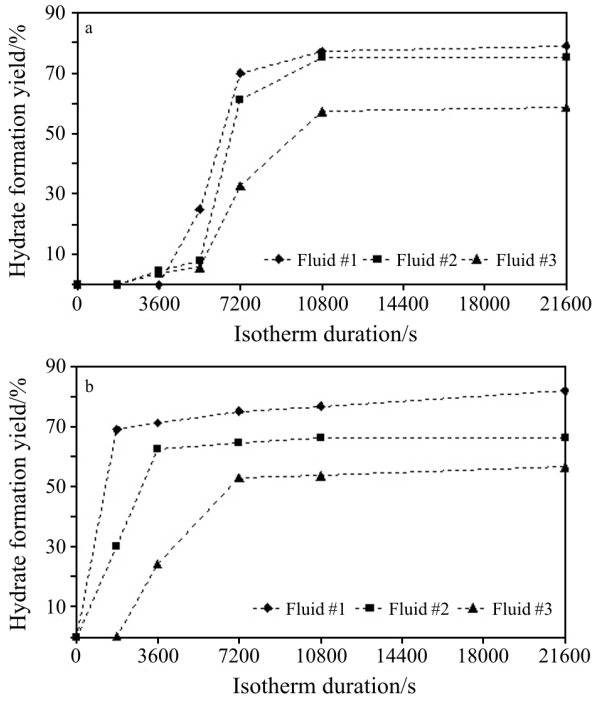

Fig. 8 Yield of hydrate formation *vs*. time at 20 K of sub-cooling, in the three drilling fluids. a – $P(CH_4)$=20 MPa; b – $P(CH_4)$=40 MPa

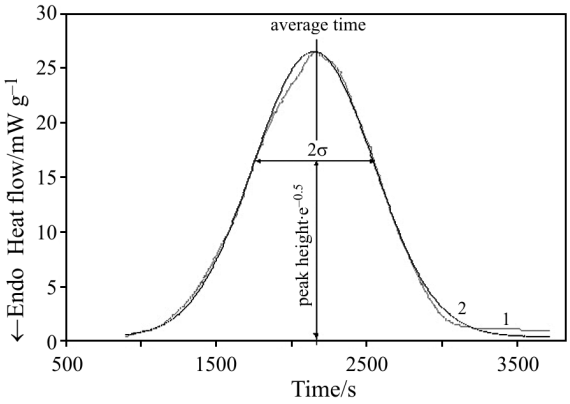

Fig. 9 1 – Peak of hydrate formation in Fig. 1 fitted by a 2 – normal statistic law (μ=2154 s, σ =400 s)

tration of calcium chloride in the fluid. This could be attributed to several causes: systematic errors in the thermodynamic model; difficulty of taking representative samples of the heterogeneous fluids; uncomplete water conversion in the brine droplets, due to either a blockage of crystal growth, or an inhibition of the nucleation. The later explanation could be related to the droplet size distribution, or the emulsion stability, which may be strongly influenced by the concentration of the brine. We are not presently able to clear this point up, and further experiments and modelling are necessary to fully elucidate the question.

Characteristic time for hydrate crystallization

As already mentioned, the heat signal of hydrate formation in emulsion is the sum of elementary heat releases accompanying the conversion of the tiny amount of water available in each droplet. We may assume that each individual crystallization occurs after a certain induction period, and has a very short duration with respect to the total duration of the peak. The overall heat release signal then represents a statistical measurement of the induction periods for the whole population of droplets. If each sample crystallizes independently of the rest of the population, the peak should fit a Gaussian, or normal, statistical law. As illustrated in Fig. 9, the hydrate formation peak of Fig. 1 may be satisfactorily represented by a normal law, following the relation:

$$\text{heat flow} = \text{baseline} + \text{peak height} \cdot \exp\left(-\frac{(t-\mu)^2}{2\sigma^2}\right)$$

The average μ of the crystallization delay of the population is given by the time abscissa t_{max} of the top of the peak. The standard deviation σ is given by the half peak width at the ordinate: baseline+peak height $e^{-0.5}$.

Several experiments were carried out at different pressures, from 7 to 32 MPa. Even though it was difficult to identify clearly the peaks of formation at the lower pressure (7 MPa), it was still possible to distinguish the time abscissa of the maximum, t_{max}, which depends on the pressure and temperature. Figure 10 presents the logarithm of the characteristic time t_{max} as a function of the inverse of the absolute temperature at which the hydrates were formed T_{iso} (K). A linear relationship, with very similar slopes, is observed for the different pressures that were studied. The larg-

Table 4 Coefficients of the linear fitting of ln t_{max} *vs.* $1/T_{iso}$ at various pressures of methane

$P(CH_4)$/MPa	7.2	13.4	22.8	32.5
A	–6210.2	–6554.8	–6406.3	–6319.1
B	33.615	34.462	33.134	32.242

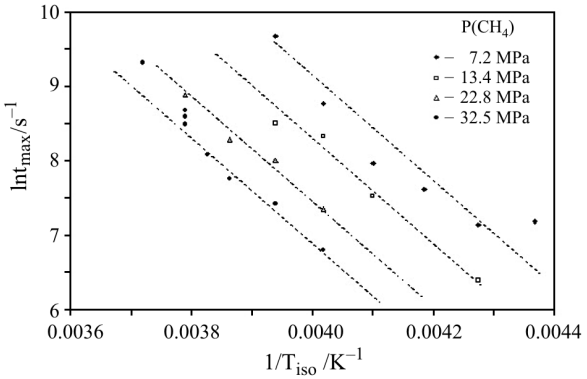

Fig. 10 lnt_{max} as a function of $1/T_{iso}$ for various methane pressures. Fluid #2

est discrepancies were found at the highest temperatures and lowest pressures, i.e. at low driving force. This may be related to the observation that the peaks of hydrate formation under low driving force fit poorly to the normal statistic law, unlike high driving force peaks. The dashed lines drawn in Fig. 10 were obtained by fitting the series of experimental points, after eliminating the most diverging points. In Table 4 are presented the coefficients *A* and *B* found for the linear relation:

$$\ln t_{max} = \frac{A}{T_{iso}} + B$$

Conclusions

High pressure DSC was applied to the study of the kinetics of formation of methane hydrates in water-in-oil emulsions. Oil-base drilling fluids designed for deep offshore drilling operations were used as the water-containing media, for the stability of these specific water-in-oil emulsions has been ascertained.

At high driving force, that is, at pressures much higher, and/or temperatures much lower than the HLV equilibrium conditions, peaks of crystallization were easily detected and could be integrated to give a representation of the rate of hydrate formation *vs.* time. At low driving force, the peak of hydrate formation is barely distinguishable. Nevertheless, the presence of hydrates is proven by the heat of dissociation, detected upon warming up the sample after the cold isotherm sequence. By repeating experiments with variable isotherm durations, it was still possible to measure the rate of hydrate formation. These experiments show that, as expected, the rate of hydrate formation increases, and the induction period duration decreases, as the degree of sub-cooling increases. However, the sub-cooling degree is not the only limiting factor, and experiments at low pressure or high temperature resulted in much slower rate of formation than expected.

High driving force formation peaks were found to fit a normal statistic law, which is characteristic of a sum of independent events. This agrees with the assumption that each water droplet in the emulsion is an independent sample that crystallizes instantaneously after an induction period. The crystallization peak is therefore a statistical representation of the induction period duration for the whole droplets population, the top of the peak giving the average duration. A relation was evidenced between the logarithm of the average time for droplet crystallization and the reverse of the absolute temperature. At lower driving force, formation peaks become less symmetrical and may no more be represented by a normal law.

The experimental method developed appears as particularly suitable for studying hydrate formation mechanisms in complex dispersed systems, where most usual methods are ineffective. The methodology based on the analysis of peaks of hydrate formation in water-in-oil emulsion during isotherms at different pressures could find many applications, such as testing the efficiency of kinetic inhibitors. The experimental results presented in this paper will be exploited in further modeling of the gas hydrates formation kinetics in drilling fluids as a function of pressure, temperature and salt concentration of the water phase, which should be useful for risk assessment in deep offshore drilling.

Acknowledgements

Authors wish to thank A. Audibert, T. Palermo, B. Herzhaft and L. Jussaume (Institut Français du Pétrole) for fruitful discussion. Contribution of Pr. D. Clausse (University of Technology of Compiègne, France) is also gratefully acknowledged.

Symbols and units

f_{CH_4}	fugacity of methane [MPa]
P	pressure [MPa]
t	time [s]
t_{max}	time abscissa of the maximum of the DSC peak during hydrate formation [s]
T	temperature [K]
T_{eq}	temperature of (hydrate+liquid+vapor) equilibrium at given gas pressure and water phase composition [K]

T_{iso} temperature of isotherm in DSC program [K]
ΔT degree of under-cooling: $T_{eq}-T_{iso}$ [K]
x mass fraction of $CaCl_2$ in the solution [mass%]
x_0 initial mass fraction of $CaCl_2$ [mass%]
x_{eq} mass fraction of $CaCl_2$ at (hydrate+liquid+vapor) equilibrium [mass%]
μ mean time for crystallization of the droplets' population [s]
σ standard deviation of the time for crystallization of the droplets' population [s]

References

1 Y. P. Handa, J. Chem. Thermodyn., 18 (1986) 891.
2 Y. P. Handa, J. Chem. Thermodyn., 18 (1986) 915.
3 S. P. Kang, H. Lee and B. J. Ryu, J. Chem. Thermodyn., 33 (2001) 513.
4 C. A. Koh, R. E. Westacott, W. Zang, K. Hirachand, J. L. Creek and A. K. Soper, Fluid Phase Equil., 194–197 (2002) 151.
5 D. Clausse, J. Dispersion Sci. Technol., 20 (1999) 315.
6 B. Fouconnier, Ph.D. Thesis, Université de Technologie de Compiègne, France 2002.
7 B. Fouconnier, Y. Manissol, D. Dalmazzone and D. Clausse, Entropie, 38 (2002) 72.
8 D. Dalmazzone, M. Kharrat, V. Lachet, B. Fouconnier and D. Clausse, J. Therm. Anal. Cal., 70 (2002) 493.
9 D. Dalmazzone, C. Dalmazzone and B. Herzhaft, SPE Journal, June (2002) 196.
10 B. Herzhaft and C. Dalmazzone, Proc. SPE Annual Technical Conference and Exhibition, New Orleans, Louisiana, USA, 30 September–3 October 2001.
11 C. Dalmazzone, B. Herzhaft and D. Dalmazzone, Proc. 4th Int. Conf. on Gas Hydrates, Yokohama, Japan, 19–23 May 2002.
12 C. Dalmazzone, B. Herzhaft, L. Rousseau, P. Le Parlouër and D. Dalmazzone, Proc. SPE Annual Technical Conference and Exhibition, Denver, Colorado, USA, 5–8 October 2003.
13 P. Le Parlouër, C. Dalmazzone, B. Herzhaft, L. Rousseau and C. Mathonat, J. Therm. Anal. Cal., 78 (2004) 165.
14 M. Kharrat and D. Dalmazzone, J. Chem. Thermodyn., 35 (2003) 1489.
15 D. Dalmazzone, D. Clausse, C. Dalmazzone and B. Herzhaft, Am. Mineral., 89 (2004) 1183.
16 J. P. Nguyen, Drilling, Editions Technip, Paris 1993.
17 J. W. Barker and R. K. Gomez, J. Petrol. Technol., 41 (1989) 297.
18 H. Ebeltoft, M. Yousif and E. Soergaard, Proc. SPE Annual Technical Conference and Exhibition, San Antonio, Texas, USA, 5–8 October 1997.
19 D. Power, K. Slater, C. Aldea and S. Lattanzi, Proc. AADE National Technology Conf., Houston, Texas, USA, 1–3 April 2003.
20 B. Fu, S. Neff, A. Mathur and K. Bakeev, Proc. SPE Annual Technical Conference and Exhibition, New Orleans, Louisiana, USA, 30 September–3 October 2001.
21 J. W. Mullin, Crystallization, Butterworths, London 1972.
22 B. J. Falabella, Ph.D. Diss. University of Massachussets, Amherst, USA 1975.
23 E. D. Sloan and F. Fleyfel, AIChE Journal, 37 (1991) 1281.
24 A. Vysniauskas and P. R. Bishnoi, Chem. Eng. Sci., 38 (1983) 1061.
25 P. Englezos, N. E. Kalogerakis, P. D. Dholabbai and P. R. Bishnoi, Chem. Eng. Sci., 42 (1987) 2647.
26 P. Skovborg and P. Rasmussen, Chem. Eng. Sci., 49 (1994) 1131.
27 K. Lekvam, and P. Ruoff, J. Am. Chem. Soc., 115 (1993) 8565.
28 D. Clausse, Research techniques utilizing emulsions, in Encyclopedia of Emulsion Technology, Vol. 2, Ed. P. Becher, Marcel Dekker, New York 1985, p. 77.
29 C. Dalmazzone and D. Clausse, Microcalorimetry, in Encyclopedic Handbook of Emulsion Technology, Ed. J. Sjöblom, Marcel Dekker, New York 2001, p. 327.
30 A. Audibert, C. Dalmazzone, D. Dalmazzone and C. Dewattines, Proc. SPE Annual Technical Conference and Exhibition, Houston, Texas, USA, 26–9 September 2004.
31 B. Fouconnier, Y. Manissol, D. Dalmazzone and D. Clausse, Proc. 7èmes Journées Européennes Thermodynamique Contemporaine, Mons, Belgium, 27–31 August 2001.

Received: January 26, 2006
Accepted: April 4, 2006

DOI: 10.1007/s10973-006-7518-1